## Entropy driven atomic motion in laser-excited bismuth

Y. Giret<sup>1</sup>, A. Gellé<sup>1</sup> and B. Arnaud<sup>1</sup>

<sup>1</sup>Institut de Physique de Rennes (IPR), UMR UR1-CNRS 6251,
Campus de Beaulieu - Bat 11 A, 35042 Rennes Cedex, France, EU

(Dated: October 11, 2018)

We introduce a thermodynamical model based on the two-temperature approach in order to fully understand the dynamics of the coherent  $A_{1g}$  phonon in laser-excited bismuth. Using this model, we simulate the time evolution of (111) Bragg peak intensities measured by Fritz et al [Science 315, 633 (2007)] in femtosecond X-ray diffraction experiments performed on a bismuth film for different laser fluences. The agreement between theoretical and experimental results is striking not only because we use fluences very close to the experimental ones but also because most of the model parameters are obtained from ab-initio calculations performed for different electron temperatures.

PACS numbers: 61.80.Ba, 63.20.dk, 71.15.Pd, 78.47.J-

The development of optical pump-probe experiments has revolutionised physics by allowing the study of non-equilibrium processes on a femtosecond time scale. Indeed, an ultrashort laser pulse can cause dramatic changes in the physical properties of covalently bonded solids and induce ultrafast melting, phase transitions or coherent phonons[1]. Coherent excitation of optical phonons is a general phenomenon which has been extensively investigated in bismuth where the reflectivity change following electronic excitations exhibits damped oscillations arising from atomic motions corresponding to the  $A_{1q}$  mode[2]. Unfortunately, it is not possible to directly relate the amplitude of the reflectivity signal to the atomic positions. The goal of measuring atomic position as a function of time remained elusive until the breakthrough of time resolved X-ray diffraction experiments which allow atomic motions to be followed stroboscopically with picometer spatial and femtosecond temporal resolution[3]. Different femtosecond X-ray diffraction experiments have been conducted to probe the dynamics of the  $A_{1q}$  phonon in laser-excited Bi[4–7]. In this letter, we try to understand and to reproduce the time evolution of (111) Bragg peak intensities measured by Fritz et al[5].

Bismuth is a semi-metallic solid, whose structure can be derived from the face-centered-cubic lattice by a weak rhombohedral distorsion of the cubic unit cell. The crystal basis consists of two atoms located along the body diagonal of length c at  $\pm uc$ , where u is the  $A_{1q}$  phonon coordinate. At 300 K, the equilibrium value of u is  $u_{eq} \simeq 0.234$ [8]. It is now well established that the sudden change of  $u_{eq}$  following laser excitation explains the generation of coherent phonons in Bi. The time evolution of u can be obtained from the displacive excitation of coherent phonons (DECP) model[2]. This model, based on the idea that  $u_{eq}$  increases linearly as a function of the excited carriers density n and that n decreases exponentially as a function of time, however does not capture all aspects of the phonon and electron dynamics. Two approaches based on ab-initio calculations [9, 10] have been proposed to describe the non-equilibrium electron distribution. Murray et al[9] assumed that electrons and holes can be described by two Fermi-Dirac (FD) distributions with the same temperature but different chemical potentials, and obtained a good agreement with experiments concerning the early oscillations of the  $A_{1g}$  phonon[5]. Zijlstra et al[10] studied the coupling between the  $A_{1g}$  and  $E_g$  modes and assumed that electrons and holes can be described by a unique FD distribution. They claimed that a two-chemical potential model does not provide a realistic description of the electron dynamics in Bi, at least for high fluences. While such a claim seems to be supported by recent work based on a two-fluid model[6], the relevance of the two approaches remains unclear[11, 12].

In this work, we consider a model based on the twotemperature approach[13] where the electron system is locally described by a single FD distribution, the  $A_{1g}$ phonon mode obeys a classical equation of motion and all the remaining modes are lumped in a unique phonon bath with specific heat  $C_l$ . We assume that both the electron temperature  $T_e$  and lattice temperature  $T_l$  are well defined at each time because of electron-electron and phonon-phonon interactions. Making a local energy balance, the heat respectively received by the electron and phonon systems is given by:

$$T_{e}\frac{\partial S}{\partial t} = \frac{\partial U}{\partial t} + \frac{fc}{v}\frac{\partial u}{\partial t} = P + \frac{\partial}{\partial z}\left(\kappa_{e}\frac{\partial T_{e}}{\partial z}\right) - G_{0}\left(T_{e} - T_{l}\right)$$

$$\tag{1}$$

$$C_{l} \frac{\partial T_{l}}{\partial t} = +G_{0} \left( T_{e} - T_{l} \right) + \frac{4Mc^{2}}{v\tau} \left( \frac{\partial u}{\partial t} \right)^{2}$$
 (2)

where P is the energy deposited by the laser pulse in the electron system per unit volume and time, S and U are electronic entropy and energy per unit volume, f is the force acting on the  $A_{1g}$  phonon,  $\kappa_e$  is the electron thermal conductivity,  $G_0$  is the electron-phonon coupling constant which governs the heat transfer from the electron system to the lattice, v is the unit cell volume, M is the mass of a Bi atom and  $\tau$  is the lifetime of the  $A_{1g}$  phonon. Since the laser spot diameter is much larger than the penetration depth we only consider the spatial dependence of the parameters in the direction perpendicular to the surface, labelled as z. One should notice that

all parameters of Eq. 1 and 2 depend on  $T_e$  and u, both of which depend on the depth z. These equations have to be solved together with the phonon equation of motion:

$$\frac{\partial^2 u}{\partial t^2} = \frac{f}{2Mc} - \frac{2}{\tau} \frac{\partial u}{\partial t} \tag{3}$$

where the last term describes the energy transfer from the coherent phonon to the incoherent phonon bath, and where the force f is defined by:

$$f = -\frac{v}{c} \left. \frac{\partial U}{\partial u} \right|_{S}. \tag{4}$$

In order to evaluate the force f acting on the coherent phonon and other quantities involved in our model, we performed ab-initio calculations for different electron temperatures  $T_e$  and phonon coordinates u. All these calculations were done within the framework of the local density approximation (LDA) for the exchangecorrelation functional to density functional theory (DFT) using the ABINIT code[14]. Spin-orbit coupling was included and an energy cut-off of 15 Hartree in the planewave expansion of wavefunctions together with a  $12 \times 12 \times 12$  kpoint grid for the Brillouin zone integration were used. These parameters ensure the convergence of both vibrational and electronic properties [15]. The experimental lattice parameters at room temperature are used[8] and volume changes due to an increase of the lattice temperature  $T_l$  are neglected.

First, we calculated both energy U and entropy S as a function of u and  $T_e$  and hence obtained U(S, u). Figure 1.a shows that the equilibrium position  $u_{eq}$  increases from 0.233 to 0.25 as S increases from 0 to  $\sim 2.0~{\rm k}_B$  per unit cell. This finding confirms the displacive mechanism of phonon generation and is qualitatively in line with the behaviour observed by Murray et al[9] using a two chemical potential approach or by Zijlstra et al[10] using the same type of approach as in the work reported here. If we assume that the laser pulse energy is deposited homogeneously at the end of the pulse  $(\kappa_e \to \infty)$ , Eq. 1 shows that the electronic entropy S becomes a constant of motion provided that the energy transfer from the electron system to the lattice is frozen  $(G_0 = 0)$ . The solution of Eq. 3 when  $\tau \to \infty$  (undamped dynamics) then provides the phonon frequency  $\nu$  of the  $A_{1g}$  mode for a given entropy S which depends on the laser pulse fluence. Figure 1.b shows that  $\nu$  decreases from 2.93 Thz to 0 Thz when S increases from 0 to  $\sim 1.37 \text{ k}_B$  per unit cell. This red shift is still in qualitative agreement with previous theoretical studies[9, 10].

We have also calculated the lattice specific heat  $C_l$  within the harmonic approximation[16]. As shown in Fig. 1.c, the agreement between our calculated lattice specific heat and the experimental data[17] is good up to  $T_l \sim 300$  K. The discrepancies between theoretical and experimental results become larger at higher temperature because of anharmonic interactions neglected in our calculation. In our simulations, the initial lattice temperature  $T^0$  was

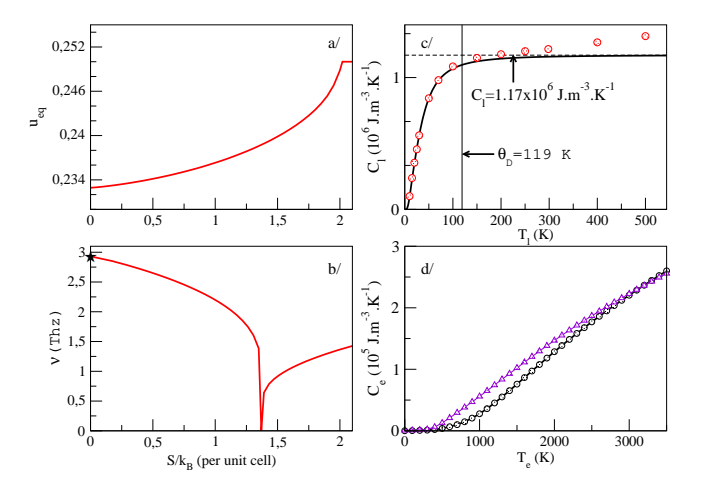


FIG. 1: (color online) a/ $u_{eq}$  as a function of electronic entropy S. b/ $A_{1g}$  phonon frequency  $\nu$  (in Thz) as a function of S. The star indicates the Raman frequency measured at 300 K[17]. c/ The calculated constant-volume lattice specific heat  $C_l$  (solid line) of Bi compared to experimental data (open circles) from Ref. [17] for lattice temperatures  $T_l$  up to the melting temperature  $T_f = 544$  K. d/ Calculated electron specific heat  $C_e$  as a function of electron temperature  $T_e$  for u=0.233 (black circles) and u=0.24 (violet triangles).

set to 300 K. As  $T^0 \gg \theta_D$  where  $\theta_D = 119$  K is the Debye temperature, the temperature dependence of  $C_l$  can be neglected. Indeed,  $C_l(T^0)$  is only 1 % smaller than the value given by the Dulong-Petit law shown as a dashed line in Fig. 1.c. The electron temperature dependence of  $C_l$  can also be safely neglected.

Finally, we calculated the electron specific heat of Bi,  $C_e = \partial U/\partial T_e$ , as a function of electron temperature  $T_e$  for different values of u. As expected, the temperature dependence of  $C_e$  is linear at low electron temperatures. Figure 1.d shows that a significant positive deviation from the linear behaviour occurs when  $T_e$  becomes larger than  $\sim 300$  K and that this deviation increases when u increases, i.e. when Bi goes toward the hypothetical metallic state corresponding to u = 0.25. The knowledge of  $C_e(T_e)$  is crucial, not only because it gives a correct estimate of the rise of temperature in the electron system, but also because it is related to the electron thermal conductivity  $\kappa_e$ . Indeed, assuming that the total electron scattering rate is dominated by the electron-phonon scattering rate, the electron thermal conductivity can be approximated by  $\kappa_e(T_e, T_l) = \kappa_0 \times (C_e(T_e)/C_e(T^0)) \times (T^0/T_l)[18, 19]$ where the dependence on u has been omitted and where  $\kappa_0 = 11 \text{ W.m}^{-1}.\text{K}^{-1}$  is the experimental value at room temperature[20].

We can now simulate the time-resolved X-ray diffraction experiments performed by Fritz  $et\ al[5]$  on a Bi film of thickness L=50 nm excited by a near-infrared laser pulse whose full width at half maximum (FWHM) is

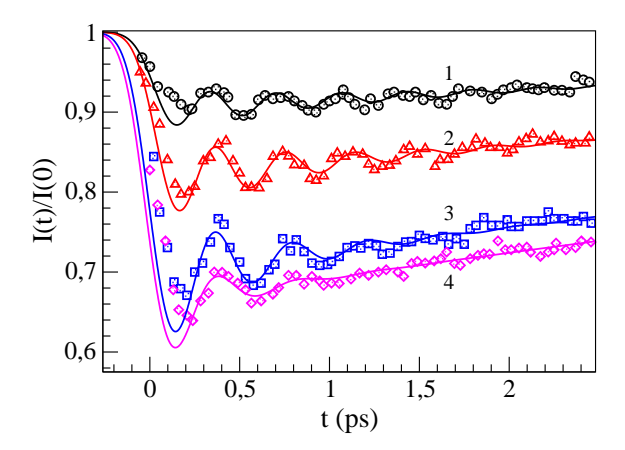


FIG. 2: (color online) Normalized intensities of the (111) Bragg peak measured by Fritz et al[5] as a function of time delay t between the laser pulse and X-ray probe for different absorbed fluences (symbols) compared to the theoretical calculation (solid lines). The measured fluences are 0.7 (black circles), 1.2 (red triangles), 1.7 (blue squares) and 2.3 mJ.cm<sup>-2</sup> (magenta losanges). The parameters used in our simulations are given from top to bottom for curves labelled 1 to 4: the absorbed fluences  $F_{abs}$  are 0.64 (black),  $1.26 \text{ (red)}, 2.18 \text{ (blue)} \text{ and } 2.47 \text{ mJ.cm}^{-2} \text{ (magenta)}; \text{ The ef-}$ fective electron-phonon coupling constants  $G_0$  are 0.84, 1.15, 1.40 and  $1.45\times10^{16}~\mathrm{W.m^{-3}.K^{-1}}$  and the decay times  $\tau$  are 0.87, 0.64, 0.44 and 0.25 ps respectively. The uncertaintities for  $\tau$  are quite large for curves 1 and 2 because of the limited duration of the experiments. The fitted value of the FWHM of the X-ray pulses is  $t_X = 205$  fs.

 $t_w = 70$  fs. The source term P(z,t) in Eq. 1 is given by:

$$P(z,t) = \frac{2F_{abs}}{l_p t_w} \sqrt{\frac{\ln 2}{\pi}} \exp\left[-4\ln 2\frac{t^2}{t_w^2}\right] \exp\left[-\frac{z}{l_p}\right] \quad (5)$$

where  $l_p = 14$  nm is the penetration depth at wavelength of 800 nm[17] and  $F_{abs}$  is the absorbed fluence. The solution of the coupled differential equations 1, 2 and 3 for a set of the two unknown physical parameters  $G_0$  and  $\tau$ , which are assumed to remain constant on the time scale of the experiment for a given fluence, provides u(z,t) and  $T_e(z,t)$ . As will be seen later, the spatial dependence of u and  $T_e$  can be neglected only  $\sim 100$  fs after the arrival of the laser pulse on the Bi surface. Therefore, the normalized intensity of the (111) Bragg peak is given by  $I(t)/I(0) = \cos^2[6\pi u(t)]/\cos^2[6\pi u(0)]$  and is convoluted with a Gaussian with FWHM  $t_X$  to account for the temporal resolution of the experiment[5]. The results of a least-squares fit of our model to the experimental data are shown as solid curves in Fig. 2 for four absorbed fluences. The parameters  $F_{abs}$ ,  $G_0$ ,  $\tau$  and  $t_X$  are given in the caption. The absorbed fluences used in our calculations are very close to the experimental fluences with the largest deviation occurring for the curve labelled 3 in Fig. 2. The electron-phonon coupling constant  $G_0$ increases from 0.84 to  $1.45\times10^{16}$  W.m<sup>-3</sup>.K<sup>-1</sup> and the decay time  $\tau$  of the coherent phonon decreases from 0.87

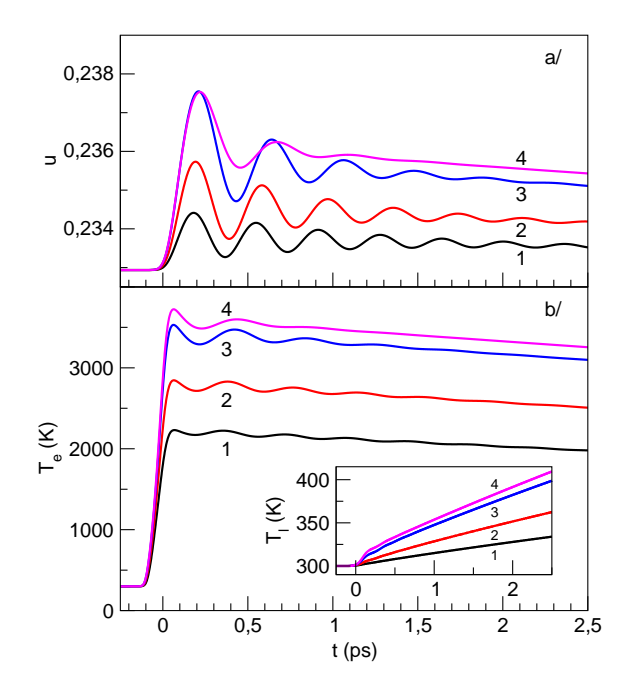


FIG. 3: (color online) a/u as a function of time delay t for the parameters given in the caption of Fig. 2. b/Electron temperature  $T_e$  as a function of time delay t. The inset displays the variation of the lattice temperature  $T_l$  as a function of t. The curves labelled 1 to 4 are related to the curves with the same label in Fig. 2.

to 0.25 ps as the theoretical fluence increases from 0.64 to 2.47 mJ.cm<sup>-2</sup>. The reported electron-phonon coupling constants are small compared to usual values in metals[18] because the density of states at the Fermi level is very small for Bi. Figure 2 shows that the oscillations of the (111) Bragg intensities are nicely reproduced by our quasi-isentropic model with the exception of curve 3, where  $F_{abs}$  is overestimated with respect to the experimental fluence. It is worth remarking that curves 3 and 4 are very close to each other while the experimental fluences differ by 0.6 mJ.cm<sup>-2</sup>. Interestingly, an upward shift of curve 3 by about 0.05 leads to a better agreement with our theoretical intensity for a fluence  $F_{abs}$ =1.79 mJ.cm<sup>-2</sup> very close to the experimental one.

One can now discuss the physical processes playing a role in the generation of coherent phonons. The laser energy is initially deposited in the electron system since the laser pulse duration is much shorter than the characteristic time for the electron-lattice energy exchange. At the same time, the heat diffuses in the electron system. The diffusivity  $\chi$  is approximately constant and given by  $\kappa_0/C_e(T^0) \simeq 100 \text{ cm}^2.\text{s}^{-1}$ . Therefore, the usual electron heat transport occurs and the time needed to uniformize the electron temperature  $T_e$  is roughly given by  $L^2/\chi \sim 250$  fs. Our simulations show that the spatial variations of  $T_e$ , S and u can be safely neglected only 100 fs after the laser pulse maximum. The strong overheating of the

electron system at the end of the laser pulse is illustrated in Fig. 3.b. The electron temperature reaches 2231 K for the lowest fluence and 3724 K for the highest fluence. The corresponding increases of electronic entropy S are respectively 0.39 and 0.98  $k_B$  per unit cell. As shown in Fig. 1.a, the increase in entropy leads to an increase in  $u_{eq}$ . The atoms thus start to oscillate around a new equilibrium position which evolves slowly as a function of time t due to heat transfer from the electron system to the lattice. The damped oscillations of the reduced coordinate u as a function of time delay t are shown in Fig. 3.a. The initial red-shift of the phonon frequency  $\nu$ as the fluence increases is clearly visible and can be attributed to the decrease of  $\nu$  as S increases (see Fig. 1.b). Figure 3 also shows that the oscillations of the phonon coordinate u are accompanied by oscillations in the electron temperature  $T_e$  whose amplitude and damping grow with fluence. The oscillations in  $T_e$  and u are in antiphase with respect to each other. Such a behaviour is easy to understand if one assumes that the electron subsystem undergoes an isentropic transformation  $(G_0 \to 0)$ . As the metallicity of Bi is enhanced when u increases, the electronic entropy S at constant electron temperature would increase up to a maximum value for the largest value of u. In order to compensate for the increase of S,  $T_e$  decreases and reaches its minimum value when u reaches its maximum value. Thus,  $T_e$  oscillates at the same frequency as u but in antiphase. Interestingly, such a behaviour parallels that of a gas enclosed in an insulating piston chamber. Assuming that the gas undergoes an isentropic transformation, the piston when displaced from it's equilibrium position, performs an oscillatory motion while the gas temperature undergoes a similar oscillatory motion, but in antiphase. In Bi, the electronic entropy S does not remain constant after the arrival of the laser pulse but

decays slowly due to energy exchange between the electron and lattice subsystems. The inset of Fig. 3.b shows the evolution of the lattice temperature  $T_l$  as a function of time delay t. On the time scale of the experiments ( $\sim 2.5$  ps), the increase in  $T_l$  ranges from 34 K for the lowest fluence to 110 K for the highest fluence. Although the increase of the lattice temperature is significant for the highest fluence, volume changes are expected to be delayed as illustrated by the shift in the Bragg angle occuring on a time scale of  $\sim 20$  ps in experiments[5]. It's thus reasonable to assume that the lattice parameters remain constant in our simulations.

In conclusion, we have developed a thermodynamical model in order to simulate the time evolution of the  $A_{1q}$ phonon coordinate following the arrival of a laser pulse of a given fluence on a Bi film. The intensities of the (111) Bragg peak measured by Fritz et al[5] are fairly well reproduced by our model for fluences very close to the experimental ones. This success is noteworthy since the force acting on the coherent phonon as well as most of the model parameters are obtained from ab-initio calculations. The only adjustable parameters are the effective electron-phonon coupling constant  $G_0$  and the scattering time  $1/\tau$  of the coherent phonon. Our results show that (1) both parameters increase as the fluence increases, (2) the electronic heat diffusion is crucial and (3) the oscillations of the coherent phonon are accompanied by an oscillation in the electron temperature. From a fundamental point of view, this work firmly establishes that a single chemical potential approach is reliable for describing the excited electrons and provides a complete scenario for the generation of coherent phonons in Bi films.

This work was performed using HPC resources from GENCI-CINES (Grant 2010-095096). We thank K. Dunseath and H. Cailleau for useful comments.

K.H. Bennemann, J. Phys.: Condens. Matter 16, R995 (2004)

<sup>[2]</sup> H.J. Zeiger et al., Phys. Rev. B 45, 768 (1992).

<sup>[3]</sup> T. Pfeifer, C. Spielmann and G. Gerber, Rep. Prog. Phys. 69, 443 (2006).

<sup>[4]</sup> K. Sokolowski-Tinten et al., Nature 422, 287 (2003).

<sup>[5]</sup> D.M. Fritz et al, Science **315**, 633 (2007).

<sup>[6]</sup> S.L. Johnson et al., Phys. Rev. Lett. 100, 155501 (2008).

<sup>[7]</sup> S.L. Johnson *et al.*, Phys. Rev. Lett. **102**, 175503 (2009).

<sup>[8]</sup> D. Schiferl and C.S. Barrett, J. Appl. Cryst. 2, 30 (1969).

<sup>[9]</sup> E.D. Murray, D.M. Fritz, J.K. Wahlstrand, S. Fahy and D.A. Reis, Phys. Rev. B 72, 60301 (2005).

<sup>[10]</sup> E. S. Zijlstra, L. L. Tatarinova, and M. E. Garcia, Phys. Rev. B 74, 220301 (2006).

<sup>[11]</sup> E. S. Zijlstra, L.E. Díaz-Sánchez, and M. E. Garcia, Phys. Rev. Lett. 104, 029601 (2010).

<sup>[12]</sup> S.L. Johnson et al., Phys. Rev. Lett. 104, 029602 (2010).

<sup>[13]</sup> M. I. Kaganov, I. M. Lifshitz and L. V. Tanatarov, Zh. Eksp. Teor. Fiz. 31, 232 (1956) [Sov. Phys. JETP 4, 173 (1957)].

<sup>[14]</sup> X. Gonze et al, Computer Phys. Commun. 180, 2582 (2009).

<sup>[15]</sup> L.E. Díaz-Sánchez, A.H. Romero, and X. Gonze, Phys. Rev. B 76, 104302 (2007).

<sup>[16]</sup> L.E. Díaz-Sánchez, A.H. Romero, M. Cardona, R.K. Kremer and X. Gonze, Phys. Rev. Lett. 99, 165504 (2007).

<sup>[17]</sup> American institute of Physics Handbook, 3rd ed., edited by D.E. Gray (McGraw-Hill, New York, 1972).

<sup>[18]</sup> Z. Lin, L.V. Zhigilei and V. Celli, Phys. Rev. B 77, 075133 (2008).

<sup>[19]</sup> A.P. Kanavin et al, Phys. Rev. B 57, 14698 (1998).

<sup>[20]</sup> C.F. Gallo, B.S. Chandrasekhar, and P.H. Sutter, J. Appl. Phys. 34, 144 (1963).